Molecular Dynamics and Experimental Study of Conformation Change of Poly(N-isopropylacrylamide)-hydrogels in Mixtures of Water and Methanol

Jonathan Walter,[†] Jan Sehrt,[†] Jadran Vrabec,[‡] and Hans Hasse[*,†]

Laboratory of Engineering Thermodynamics, University of Kaiserslautern, Kaiserslautern, Germany, and Thermodynamics and Energy Technology, University of Paderborn, Paderborn, Germany

E-mail: hans.hasse@mv.uni-kl.de

[*]To whom correspondence should be addressed
[†]University of Kaiserslautern
[‡]University of Paderborn

Abstract

The conformation transition of poly(N-isopropylacrylamide) hydrogel as a function of the methanol mole fraction in water/methanol mixtures was studied both experimentally and by atomistic molecular dynamics simulation with explicit solvents. The composition range in which the conformation transition of the hydrogel occurs was determined experimentally at 268.15, 298.15 and 313.15 K. In these experiments cononsolvency, i.e. collapse at intermediate methanol concentrations while the hydrogel is swollen in both pure solvents, is observed at 268.15 and 298.15 K. The composition range in which the cononsolvency is present does not significantly depend on the amount of cross-linker. The conformation transition of the hydrogel is caused by the conformation transition of the polymer chains of its backbone. Therefore, conformation changes of single backbone polymer chains are studied by massively parallel molecular dynamics simulations. The hydrogel backbone polymer is described with the force field OPLS-AA, water with the SPC/E model and methanol with the model of the GROMOS-96 force field. During simulation, the mean radius of gyration of the polymer chains is monitored. The conformation of the polymer chains is studied at 268, 298 and 330 K as a function of the methanol mole fraction. Cononsolvency is observed at 268 and 298 K which is in agreement with the present experiments. The structure of the solvent around the hydrogel backbone polymer is analysed using H-bond statistics and visualization. It is found that cononsolvency is caused by the fact that the methanol molecules strongly attach to the hydrogel's backbone polymer, mainly with their hydroxyl group. This leads to the effect that the hydrophobic methyl groups of methanol are oriented towards the bulk solvent. The (hydrogel + solvent shell) appears, hence, hydrophobic and collapses in water-rich solvents. As more methanol is present in the solvent, the effect disappears again.

Keywords: cononsolvency, hydrogen bonds, force field, molecular model, degree of swelling, polymer

Introduction

Hydrogels are three-dimensional hydrophilic polymer networks. Their most characteristic property is their swelling in aqueous solutions. Hydrogels are used in many applications. Super absorbers, such as in diapers[1] and contact lenses,[2] are well established examples. Other interesting applications like in drug delivery systems,[3] tissue engineering,[4] micro actuators[5] or epicardial restraint therapies,[6] are discussed. To fully exploit the potential of hydrogels, it is crucial to understand, describe and predict their swelling behavior.

The hydrogel which was studied in the present work is built up of poly(N-isopropylacrylamide) (PNIPAAm) and is cross-linked with N,N'-methylenebisacrylamide (MBA). PNIPAAm is one of the most extensively studied hydrogels in the scientific literature and is mainly used in bioengineering applications.[7] The degree of swelling of PNIPAAm in equilibrium is significantly influenced by the solvent type and the temperature.[8–13] Upon variation of these factors, the hydrogel typically shows a region where it is swollen and a region where it is collapsed. In between those two regions lies the region of conformation transition.

Amiya et al.[11] measured the degree of swelling of PNIPAAm hydrogels as a function of the methanol mole fraction in water/methanol mixtures at 273.15, 295.15 and 315.15 K. Mukae et al.[12] measured the same properties at 298.15 K, Althans et al.[14] at seven different temperatures between 298.15 and 308.15 K. These studies show that the hydrogel is collapsed at 315.15 K in pure water and swollen in pure methanol. For all other studied temperatures, the hydrogel is swollen in both pure solvents, but shows a region in which it is collapsed at intermediate methanol concentrations. This phenomenon is termed cononsolvency.

For systems with PNIPAAm polymers, cononsolvency was discussed in several studies.[15–17] Winnik et al.[17] investigated this phenomenon by means of the lower critical solution temperature (LCST) of the PNIPAAm polymer in water/methanol mixtures as a function of the methanol concentration.

The reasons for cononsolvency are discussed differently by different authors.[12,15,17–19] In order to explain the different conformations of PNIPAAm in water/methanol mixtures, the behavior of the

solvent molecules in the hydration shell of the polymer or hydrogel was studied by monitoring the H-bonds or the interactions between the polymer and the two solvents with different experimental methods.

Mukea et al.[12] investigated PNIPAAm hydrogels in water/alcohol mixtures at 298.15 K. They measured the H-bonds between the hydrogel and the solvents with FTIR spectroscopy and found that the hydrogel is strongly dehydrated in the collapsed state. Therefore, the hydrogel mainly interacts with itself when collapsed. Further, they measured a higher amount of alcohol in the hydrogel than in the bulk solvent, leading to a higher degree of swelling in several pure alcohols than in pure water at 298.15 K. This leads to the conclusion that methanol is the better solvent. Mukea et al.[12] also found that the interactions between water and methanol are stronger than the ones between methanol and PNIPAAm when the hydrogel is collapsed. They compared the conformation transition with the partial molar volume of methanol in water/methanol mixtures, observing a minimum at approximately the same solvent composition and assumed a relation between these properties.

In contradiction to these results, Cheng et al.,[19] using Laser light scattering and FTIR, only found a weak decrease of the number of H-bonds when the polymer collapses in pure water above the LCST.

Winnik et al.[17] investigated cononsolvency for PNIPAAm polymers in water/methanol mixtures at different temperatures. Using turbidity measurements, they found a flexible PNIPAAm coil in methanol and a stiffer and more elongated PNIPAAm coil in water. This leads these authors to the conclusion that methanol is the better solvent for PNIPAAm.

Investigating the interactions between PNIPAAm polymers and the two solvent species in water/methanol mixtures, Schild et al.[15] used infrared spectra, optical densities and calorimetry. They came to the conclusion that the relevant interactions for the conformation transition are the ones between the polymer chain and the solvent molecules.

Tanaka et al.[18] described the volume transition of PNIPAAm polymers in water/methanol mixtures based on models for cooperative and competitive hydration. They predicted a strong decrease of the H-bonds between the polymer and the solvents in the cononsolvency region and also stated that

methanol is a better solvent for PNIPAAm than water.

Molecular dynamics simulations can give a detailed insight into these phenomena on the atomistic level. The orientation of the solvents at the surface of PNIPAAm monomers in water/methanol mixtures was investigated in detail by Pang et al.[20] They found that the solvents are bound with their polar sites to the polar sites of the monomer.

In a preceding study of our group,[21] it was shown that the conformation transition of PNIPAAm upon changing the temperature can be predicted by molecular simulation. In the present work, the influence of the solvent composition on the conformation transition of PNIPAAm in water/methanol mixtures was investigated. The effect was studied both by atomistic molecular dynamics simulation and by experiment. The molecular simulations are based on the force field OPLS-AA[22,23] for PNIPAAm, SPC/E[24] for water and different explicit models from the literature for methanol. The conformation transition of the hydrogel is dominated by the interactions between the solvent molecules and the hydrogel backbone polymer.[21] Therefore, single PNIPAAm chains were investigated by molecular simulations. In these simulations, the radius of gyration and the structure of the solvent around single chains was monitored. The results are compared to the experimental data for the degree of swelling of PNIPAAm hydrogel in water/methanol mixtures as a function of the methanol mole fraction at different temperatures.

Experimental procedure and results

Chemically cross-linked hydrogels were synthesized in the present work by polymerizing N-isopropylacrylamide (NIPAAm) and by cross-linking it with N,N'-methylenebisacrylamide (MBA). The experimental method is only briefly described here as it is the same that was described earlier by Hüther and Maurer.[9] Polymerization and cross-linking were simultaneously carried out by free radical polymerization in oxygen-free deionized water at 298.15 K under nitrogen atmosphere. The reactions were initiated by small amounts of ammonium peroxodisulfate (starter) and sodium disulfite (accelerator).

For the synthesis, the monomer NIPAAm (Aldrich, 97 %, CAS 2210-25-5), the cross-linking agent MBA (Fluka, $\geq$ 99 %, CAS 110-26-9), and the initiators ammonium peroxodisulfate ($(NH_4)_2S_2O_8$) (Aldrich, $\geq$ 98 %, CAS 7727-54-0) and sodium disulfite ($Na_2S_2O_5$) (Fluka, $\geq$ 98 %, CAS 7681-57-4) were used without further purification. Oxygen-free, bi-distilled water was used for synthesis. After synthesis, the hydrogel particles were thoroughly washed with deionized water and dried in a vacuum oven.

Hydrogels can not be characterised by a few numbers like it is done with specification chemicals. They are rather characterised by their production process. The following concentrations refer to the aqueous solution in which the polymerization was carried out: Total mass fraction x^m_{gel} of polymerizable material

$$x^m_{\text{gel}} = \frac{m_{\text{NIPAAm}} + m_{\text{MBA}}}{m_{\text{total}}}, \tag{1}$$

mole fraction of cross-linking agent x^n_{MBA}

$$x^n_{\text{MBA}} = \frac{n_{\text{MBA}}}{n_{\text{NIPAAm}} + n_{\text{MBA}}}, \tag{2}$$

and mass fraction of the initiator x^m_{s}

$$x^m_{\text{s}} = \frac{m_{\text{s}}}{m_{\text{total}}}. \tag{3}$$

Here, m and n are the mass and mole number, respectively. The parameters for the two hydrogels synthesized in the present work are presented in 1. The hydrogels differ mainly in the degree of cross-linking.

For each swelling experiment, ten dried hydrogel particles were used. The amount of mass of the dried hydrogel particle was determined with a precision micro balance (type MX5, Mettler Toledo, Giessen, Germany) before the mixture of oxygen-free deionized water and methanol (Roth, 99%, CAS 67-56-1) was added to the particles. The solvent mixture was prepared with a precision balance (type XS4002S DeltaRange, Mettler Toledo, Gießen, Germany). The hydrogel in the solvent was then thermostatted for about two weeks. An air oven (type ICP 600, Memmert, Schwabach, Germany) was used at 298.15 and 313.15 K, a cryostat (type F34, Julabo, Seelbach, Germany) with

a glysantine/water mixture as coolant was used at 268.15 K. For the temperature measurement, a calibrated platinum resistance thermometer with an overall uncertainty of ± 0.1 K was used. After reaching equilibrium, the hydrogel particles were taken out of the solvent and the surface solvent was removed. The mass of the swollen particles was then determined with the precision micro balance. The degree of swelling of each particle was calculated as the ratio of mass of the swollen hydrogel m_{gel} to the mass of the dry hydrogel $m_{\mathrm{gel}}^{(\mathrm{dry})}$

$$q = \frac{m_{\mathrm{gel}}}{m_{\mathrm{gel}}^{(\mathrm{dry})}}. \tag{4}$$

For the ten particles, the arithmetic mean and the standard deviation of the degree of swelling were calculated. The experiments were performed at temperatures of 268.15, 298.15 and 313.15 K for various compositions of the water/methanol mixture. The experimental results are summarized in 2 and 3.

Discussion of experimental results

1 and 2 present experimental results for the degree of swelling of the two hydrogels in water/methanol mixtures for different temperatures as a function of the mole fraction of methanol. 1 shows the influence of the temperature on the degree of swelling of Hydrogel 1. The influence of the amount of cross-linker is discussed by directly comparing the results for Hydrogel 1 and Hydrogel 2 at 298.15 K in 2. The error bars denote the standard deviations, which are mostly within the symbol size.

The results for Hydrogel 1 are presented in 1. For all three temperatures, the hydrogel is swollen in pure methanol. The degree of swelling in pure methanol and methanol-rich mixtures is only very weakly temperature dependent. Higher temperatures lead to a lower degree of swelling. In pure water, the hydrogel is swollen at 298.15 K and collapsed at 313.15 K. At 298.15 K the hydrogel shows a stronger swelling in pure water than in pure methanol. At 268.15 K, the degree of swelling can not be measured in pure water, because it is below freezing temperature. At 268.15

and 298.15 K cononsolvency was observed: even though the hydrogel is swollen both in pure water (or water-rich mixtures at 268.15 K) and pure methanol, there is a composition range of the solvent mixture where the hydrogel is collapsed. Adding small amounts of methanol to pure water leads to a strong decrease of the degree of swelling, whereas adding small amounts of water to pure methanol has hardly any effect. There seems to be a shallow local maximum of the degree of swelling in the region of high methanol mole fractions. Thus, the cononsolvency region is observed on the water-rich side of the diagram shown in 1. In the cononsolvency region at 298.15 K, the hydrogel collapses significantly, but not to the level that is observed at the other temperatures. This is supported by the findings of Winnik et al.,[17] who reported no cononsolvency for PNIPAAm polymers in water/methanol mixtures below about 263 K.

For Hydrogel 2, the results are qualitatively the same as for Hydrogel 1. These results are presented in 3. In 2, the two hydrogels are compared for the temperature of 298.15 K. The two hydrogels mainly differ in the degree of cross-linking (cf. 1). The degree of swelling is higher for Hydrogel 1, which has a lower amount of cross-linking. The solvent composition range, in which cononsolvency was observed is hardly influenced by the degree of cross-linking. This corroborates that cononsolvency is caused by the interactions between the hydrogel backbone polymer and the solvent molecules. This is in line with the finding that the volume transition of hydrogels upon temperature change also does not significantly depend on the degree of cross-linking.[21]

The results of the swelling experiments of PNIPAAm hydrogels can be compared with the solubility experiments of PNIPAAm polymers in water/methanol mixtures by Winnik et al.,[17] where cloud points were measured. The volume transition of hydrogels and the solubility of the backbone polymer are closely related properties, as both depend on the interactions between the polymer and the solvent. A direct quantitative comparison is, however, not straightforward, especially as the volume transition of the hydrogel does not take place at a specific composition, but rather over a composition range that may be wide. In the present work, an empirical approach was followed to achieve a mapping. The crucial step in that approach is to determine a certain solvent composition "at which the volume transition occurs" from the hydrogel swelling data. In reality, there is rather

a composition range, such that a specific methanol mole fraction has to be chosen suitably by a well defined procedure which will, however, unavoidably be somewhat arbitrary.

For the definition of that "transition point", in the present work, the degree of swelling at that point q^* was specified and then the composition of the transition point $x^{n,*}_{\mathrm{MeOH}}$ was determined from the plot of $q(x_{\mathrm{MeOH}})$, cf. 1 and 2. For that definition of q^*, the minimum of q observed at 268.15 K was selected (Hydrogel 1: 8.5 g·g^{-1}, Hydrogel 2: 9.5 g·g^{-1}). The temperature of 268.15 K is close to the lowest temperature of the cloud point curve observed by Winnik et al.[17] so that no full collapse was observed. Note also that q^* for Hydrogel 1 corresponds to a transition temperature $T^* = 305$ K in plots of $q(T)$ for that hydrogel,[21] which is in good agreement with other data that is reported for that transition in the literature.[25,26]

The results for the transition mole fractions $x^{n,*}_{\mathrm{MeOH}}$ for different temperatures are listed in 4 and shown in 3, where they are compared with the experimental results of Winnik et al.[17] In 3, the cloud point curve of the polymer is compared to the data estimated from the hydrogel volume transition, showing the relation between the temperature and the solvent composition at the transition points.

The comparison shows that the conditions for which the volume transition of the PNIPAAm hydrogel was observed and the cloud point of the PNIPAAm polymer are almost identical. Furthermore, it was found that the effect does not significantly depend on the amount of cross-linker. Both findings support the interpretation that the volume transition of the hydrogel is an effect related to the interactions between backbone polymer and solvent molecules.

Force fields

For the present molecular dynamics simulations of PNIPAAm in water/methanol mixtures, the OPLS-AA (OPLS) force field[22,23] was used to describe PNIPAAm. It was combined with the SPC/E water model.[24] In preceding studies,[21] it was shown that this combination is suited for predicting the conformation change of PNIPAAm in water as a function of the temperature. The

Lennard-Jones (LJ) and point charge parameters of the OPLS force field used for PNIPAAm are given in 5.

For methanol the model of GROMOS96 with low point charges (G96-low)[27] was used. The potential and geometry parameters are listed in 6 and 7, respectively. Two other methanol models (Schnabel et al.[28] and GROMOS96 with high point charges[27]) were also tested in preliminary studies, but were not found to yield cononsolvency. The results of these preliminary studies are briefly presented in Appendix A in the Supporting Information.

For the unlike LJ pair interaction, a geometric mean mixing rule for both σ and ε was used, as specified by the OPLS force field

$$\begin{aligned} \sigma_{ij} &= \sqrt{\sigma_i \cdot \sigma_j}, \\ \varepsilon_{ij} &= \sqrt{\varepsilon_i \cdot \varepsilon_j}. \end{aligned} \tag{5}$$

For the intramolecular interactions, the method of the 1-4 interactions was employed.[29] Thereby, the interactions between a given atom and its first and second neighbors were only modeled by the bond and the angle term. Interactions between the atom and its third neighbor were calculated by the dihedral, the Coulomb interaction and the LJ term. The last two terms were reduced by a scaling factor of 0.5. All other intramolecular interactions were modeled with the unmodified Coulomb interaction and LJ term.

Simulation methods

Molecular simulations of PNIPAAm single chains were carried out with version 4.0.5 of the GROMACS simulation package,[30,31] which was developed for the simulation of large molecules in solutions.

Single PNIPAAm chains in water were simulated in the isothermal-isobaric ensemble. The pressure was specified to be 1 bar and was controlled by the Berendsen barostat,[32] the temperature was

controlled by the velocity-rescale thermostat[33] and the timestep was 1 fs for all simulations. The standard deviation of the temperature over time is about 1.3 K.[21] Newton's equations of motion were numerically solved with the leap-frog integrator.[34] The cutoff radius was $r_c = 1.5$ nm for all interactions. For the long-range electrostatic interactions, particle mesh Ewald[35] with a grid spacing of 0.12 nm and an interpolation order of four was used.

The simulations were carried out with PNIPAAm chains of 30 monomers as in.[21] For setting up the starting conformation, the procedure suggested in[21] was adopted. A stretched configuration derived from a simulation of the polymer chain in pure water in equilibrium at 280 K was used. Prior to the simulations, the solvent mixtures were equilibrated using about 3500 solvent molecules over $2 \cdot 10^6$ time steps monitoring the density. The equilibrated solvent was then used to solvate the PNIPAAm chain. The simulation volume was about $14 \times 6 \times 6$ nm and contained in addition to the single PNIPAAm chain about 14000 solvent molecules. After solvent equilibration over 1 to $5 \cdot 10^6$ timesteps with a fixed polymer configuration, production runs over 2 to $8 \cdot 10^7$ time steps (20 to 80 ns) were carried out.

In order to analyze the results, the radius of gyration R_g was calculated

$$R_g = \left(\frac{\Sigma_i ||\mathbf{r}_i||^2 m_i}{\Sigma_i m_i} \right)^{1/2}, \tag{6}$$

which characterizes the degree of stretching of the chain, where m_i is the mass of site i and $||\mathbf{r}_i||$ is the norm of the vector from site i to the center of mass of the chain. The radius of gyration in equilibrium was calculated as the arithmetic mean over the last 10^7 time steps of the run (1000 samples) together with its standard deviation.

In order to investigate the structure of the solvent species around the PNIPAAm chain, the average number of H-bonds between the polar amide group of the chain and the solvent molecules was measured. For identifying H-bonds, a geometric criterion was employed which is based on the distance between acceptor and donor and the angle acceptor-donor-hydrogen. A H-bond was assumed to be present, if the distance is below 0.3 nm and the angle smaller than 30°.[36,37]

For further information about the structure of the solvent around the PNIPAAm chains, in some simulations, the backbone of the single chain was visualized together with the solvent molecules of the hydration shell using VMD[38] and MegaMol.[39,40]

The simulations were performed on the high performance computer HP XC 4000 at the Steinbuch Centre for Computing in Karlsruhe (Germany), which is equipped with Opteron 2.6 GHz Dual Core processors. In typical runs, 128 cores were used. Preliminary studies of strong scaling of GROMACS on that hardware show that the program can be used efficiently up to about that number of processors.[41] Typical runs consumed about 18000 CPU h.

Simulation results

Simulations of PNIPAAm chains of 30 monomers in water/methanol mixtures of different compositions were carried out at 268, 298 and 330 K to determine the radius of gyration of the polymer in equilibrium. The simulation results are summarized in 8 and presented graphically in 4 which shows the radius of gyration in equilibrium as a function of the mole fraction of methanol.

The results at 268 K are presented in the top panel of 4. In pure methanol and in water-rich mixtures, the single chain is stretched. There is no data for pure water because it is solid at this temperature. The results show a small region of cononsolvency at methanol mole fractions of about 0.6 mol·mol^{-1}. The observation of cononsolvency at this temperature is in agreement with the experimental data, even though the composition range in which cononsolvency occurs is not correctly predicted. The experiments from the present work on PNIPAAm hydrogels as well as the experimental results on PNIPAAm polymers of Winnik et al.[17] indicate that cononsolvency does not exist at temperatures substantially below 268 K. The simulation result with the small cononsolvency region at 268 K is in line with these observations.

The central panel of 4 shows the results at 298 K. Again, in both pure solvents, the single chain is stretched, for intermediate methanol mole fractions between 0.1 and 0.2 mol·mol^{-1} it is collapsed. The region of cononsolvency is predicted to be much larger than at 268 K and is now in the com-

position range in which it was also observed experimentally, cf. 1.

The results at 330 K are presented in the bottom panel of 4. In pure water, the single chain is collapsed, in pure methanol, it is stretched. In the mixture, at methanol mole fractions above about 0.6 mol·mol^{-1}, the chain is stretched. This is in fair agreement with the results obtained with the present experiments at the highest studied temperature of 313 K, cf. 1. These temperatures are compared with each other because they are both somewhat above the transition temperature in pure water, which is about 305 K determined by experiment and about 320 K determined by molecular simulation.[21]

These results show that it is possible to qualitatively predict the volume transition of hydrogels by molecular simulation if suitable force fields are chosen. This is encouraging as the underlying force fields were developed using only information which is unrelated to the phenomenon studied here and no further adjustments were made.

However, molecular simulation offers more than just the possibility to predict the volume transition. The extremely highly resolved information provided by such simulations allows gaining insight into the reasons of cononsolvency. For that purpose, the structure of the solvent around the PNIPAAm chain was studied both by H-bond statistics and visualization.

The number of H-bonds between the two solvent species and the amide groups of the PNIPAAm chain was determined for the equilibrated chain. The H-bonds form between the oxygen atom of the amide group and the hydrogen atoms of the solvents as well as between the hydrogen atom of the amide group and oxygen atom of the solvents (cf. Appendix B in the Supporting Information). In principle, also the nitrogen atom of the amide group of PNIPAAm may act as H-bond acceptor. The results obtained in the present study show that the number of H-bonds that involve this nitrogen atom is so small that it can be neglected. They also show that the amount of intramolecular H-bonding of the PNIPAAm chain is small compared to the number of intermolecular H-bonds between the chain and the solvent molecules. Thus intramolecular H-bonding is neglected in the following. The low number of intramolecular H-bonds may be due to the chain length chosen in the present study, but the same results were also found for longer chains and three dimensional

networks that were also simulated here.

5 shows the average number of H-bonds between a monomer unit of the PNIPAAm chain and water or methanol, respectively, as a function of the methanol mole fraction at 298 K. For comparison, the radius of gyration of the single chain is plotted as well. Furthermore, 5 contains linear interpolations between the number of H-bonds in the two pure solvents and zero for the case in which the solvent is not present. It can be seen that less H-bonds are present in pure methanol than in pure water, which is related to the stronger stretching of the chain in water than in methanol. But despite this, in mixtures of these solvents, the PNIPAAm chain has a stronger preference for forming H-bonds with methanol than with water. Considering the entire composition range from pure water to pure methanol, the number of H-bonds with methanol increases more than linearly while the number of H-bonds with water decreases more than linearly. Thus, the number of H-bonds of the PNIPAAm chain with methanol exceeds the number of H-bonds with water already at methanol mole fractions of about 0.15 mol·mol^{-1}. The occurrence of cononsolvency upon increasing the methanol mole fraction goes along with a strong decrease of the number of H-bonds between water and the PNIPAAm chain and a strong increase of the corresponding H-bonds with methanol.

These results confirm that methanol is a better solvent for PNIPAAm than water. The PNIPAAm chain is collapsed in the region where the methanol concentration around PNIPAAm strongly differs from that in the bulk solvent. This indicates that the collapse of the polymer or hydrogel is related to interactions between the solvation shell around PNIPAAm and the rest of the solvent. This finding is in agreement with the conclusions Schild et al.[15] drew from their experimental studies of PNIPAAm polymers and hydrogels.

In 9, the average number of H-bonds between the two solvent species and the oxygen and hydrogen atom of the amide group of PNIPAAm are presented for a methanol mole fraction in the solvent of 0.1 mol·mol^{-1}, which is inside the cononsolvency region. From these results, it can be seen that water is preferably attached to the oxygen atom and methanol to the hydrogen atom of the amide group. The hydrogen atom is further away from the backbone of the PNIPAAm chain than the

oxygen atom (cf. 6). Therefore, water within the solvation shell is preferably closer to the backbone, while methanol resides preferably in the outer regions of the solvation shell. Furthermore, methanol is attached with its polar hydroxyl group to the amide group so that its non-polar methyl group is oriented towards the bulk solvent. This is in good agreement with findings of Pang et al.[20] who investigated the orientation of methanol and water at PNIPAAm monomers in water/methanol mixtures with molecular dynamics simulation in detail.

For the following discussion, it is assumed that the PNIPAAm chain together with its solvation shell can be considered as an entity, a standpoint which is supported by the strong H-bonding between the solvation shell and the chain and also by visualizations of the molecular trajectory. Due to the effect described above, the PNIPAAm chain + solvation shell has a hydrophobic methyl-rich surface. It is presumed that this leads to a solubility mismatch with water-rich bulk solvents and consequently the collapse of the hydrogel or the precipitation of the polymer in the region of cononsolvency. With increasing methanol mole fraction, the bulk solvent becomes more compatible with the hydrophobic PNIPAAm chain + solvation shell, leading to the disappearance of cononsolvency.

More detailed information on H-bonding statistics is given in Appendix B in the Supporting Information. The Appendix also contains information on the visualization of the simulation results, some of which are made available in the Supplementary Material of the present work.

Conclusion

The dependence of the volume transition of PNIPAAm hydrogels on the composition of the solvent in water/methanol mixtures was studied both experimentally and by molecular simulation. Cononsolvency was observed with both approaches. The region in which it occurs in the experimental studies of hydrogels is almost independent of the amount of cross-linking, which indicates that the effect is related to the interactions between the hydrogel backbone polymer and the solvent.

Therefore, single polymer chains in explicit solvents were studied by molecular simulation. Force

fields from the literature for the polymer chain, water and methanol were selected that are capable to predict cononsolvency. The region, in which it occurs, is qualitatively and sometimes even quantitatively predicted by the simulations without adjusting any parameters.

The simulation results indicate that the reason for cononsolvency is the strong H-bonding between methanol and the PNIPAAm chain, which leads to a preferred molecular orientation of methanol, where the methyl group points towards the bulk solvent. The PNIPAAm chain + solvation shell entity therefore has a hydrophobic methyl-rich surface. This leads to mismatch with water-rich bulk solvents and consequently to the collapse of the hydrogel or the precipitation of the polymer in the region of cononsolvency.

Acknowledgement

We gratefully thank the German Research Foundation (DFG) for funding support within the Collaborative Research Centre 716. The computer simulations were performed on the high performance computer HP XC 4000 of the Steinbuch Centre for Computing in Karlsruhe (Germany) under the project LAMO. We also thank Thomaß Bertram, Sebastian Grottel and Guido Reina from the Institute for Visualization and Interactive Systems at the University of Stuttgart (Germany) for their support with respect to visualization. The work was carried out under the auspices of the Boltzman-Zuse Society for Computational Molecular Engineering.

Supporting Information Available

In the Supplementary Material visualizations of the solvent structure around the PNIPAAm chains are contained (cf. Appendix C in the Supporting Information). Three visualizations show the structure and H-bonds of the solvents at different solvent compositions. The fourth visualization shows the local concentration of the solvents around the PNIPAAm chain in the cononsolvency region and the collapse of the chain. This material is available free of charge via the Internet at http://pubs.acs.org.

References

(1) El-Rehim, H. A. A. *Radiat. Phys. Chem.* **2005**, *74*, 111–117.

(2) Pavlyuchenko, V. N.; Sorochinskaya, O. V.; Ivanchev, S. S.; Khaikin, S. Y.; Trounov, V. A.; Lebedev, V. T.; Sosnov, E. A.; Gofman, I. V. *Polym. Adv. Technol.* **2009**, *20*, 367–377.

(3) Peppas, N.; Bures, P.; Leobandung, W.; Ichikawa, H. *Eur. J. Pharm. Biopharm.* **2000**, *50*, 27–46.

(4) Slaughter, B. V.; Khurshid, S. S.; Fisher, O. Z.; Khademhosseini, A.; Peppas, N. A. *Adv. Mater.* **2009**, *21*, 3307–3329.

(5) van der Linden, H.; Olthuis, W.; Bergveld, P. *Lab Chip* **2004**, *4*, 619–624.

(6) Fujimoto, K. L.; Ma, Z.; Nelson, D. M.; Hashizume, R.; Guan, J.; Tobita, K.; Wagner, W. R. *Biomaterials* **2009**, *30*, 4357–4368.

(7) Rzaev, Z. M. O.; Dinçer, S.; Pişkin, E. *Prog. Polym. Sci.* **2007**, *32*, 534–595.

(8) Hüther, A.; Schäfer, B.; Xu, X.; Maurer, G. *Phys. Chem. Chem. Phys.* **2002**, *4*, 835–844.

(9) Hüther, A.; Maurer, G. *Fluid Phase Equilib.* **2004**, *226*, 321–332.

(10) Hüther, A.; Xu, X.; Maurer, G. *Fluid Phase Equilib.* **2004**, *219*, 231–244.

(11) Amiya, T.; Hirokawa, Y.; Hirose, Y.; Li, Y.; Tanaka, T. *J. Chem. Phys.* **1987**, *86*, 2375–2379.

(12) Mukae, K.; Sakurai, M.; Sawamura, S.; Makino, K.; Kim, S. W.; Ueda, I.; Shirahama, K. *J. Phys. Chem.* **1993**, *97*, 737–741.

(13) Crowther, H.; Vincent, B. *Colloid Polym. Sci.* **1998**, *276*, 46–51.

(14) Althans, D.; Langenbach, K.; Enders, S. *Mol. Phys.* **2012**, in press, DOI: 10.1080/00268976.2012.655339.

(15) Schild, H. G.; Muthukumar, M.; Tirrell, D. A. *Macromolecules* **1991**, *24*, 948–952.

(16) Tanaka, F.; Koga, T.; Winnik, F. M. *Phys. Rev. Lett.* **2008**, *101*, 028302.

(17) Winnik, F. M.; Ringsdorf, H.; Venzmer, J. *Macromolecules* **1990**, *23*, 2415–2416.

(18) Tanaka, F.; Koga, T.; Kojima, H.; Winnik, F. M. *Macromolecules* **2009**, *42*, 1321–1330.

(19) Cheng, H.; Shen, L.; Wu, C. *Macromolecules* **2006**, *39*, 2325–2329.

(20) Pang, J.; Yang, H.; Ma, J.; Cheng, R. *J. Phys. Chem. B* **2010**, *114*, 8652–8658.

(21) Walter, J.; Ermatchkov, V.; Vrabec, J.; Hasse, H. *Fluid Phase Equilib.* **2010**, *296*, 164–172.

(22) Jorgensen, W. L.; Tirado-Rives, J. *J. Am. Chem. Soc.* **1988**, *110*, 1657–1666.

(23) Jorgensen, W. L.; Maxwell, D. S.; Tirado-Rives, J. *J. Am. Chem. Soc.* **1996**, *118*, 11225–11236.

(24) Berendsen, H. J. C.; Grigera, J. R.; Straatsma, T. P. *J. Phys. Chem.* **1987**, *91*, 6269–6271.

(25) Çaykara, T.; Kiper, S.; Demirel, G. *Journal of Applied Polymer Science* **2006**, *101*, 1756–1762.

(26) Heskins, M.; Guillet, J. E. *J. Macromol. Sci., Part A: Pure Appl. Chem.* **1968**, *8*, 1441–1455.

(27) van Gunsteren, W. F.; Billeter, S.; Eising, A.; Hünenberger, P.; Krüger, P.; Mark, A.; Scott, W.; Tironi, I. *Biomolecular Simulation: The Gromos 96 Manual and User Guide*; vdf Hochschulverlag an der ETH Zürich: Zürich, Switzerland, 1996.

(28) Schnabel, T.; Srivastava, A.; Vrabec, J.; Hasse, H. *J. Phys. Chem. B* **2007**, *111*, 9871–9878.

(29) van der Spoel, D.; Lindahl, E.; Hess, B.; van Buuren, A. R.; Apol, E.; Meulenhoff, P. J.; Tieleman, D. P.; Sijbers, A. L. T. M.; Feenstra, K. A.; van Drunen, R.; Berendsen, H. J. C. Gromacs User Manual version 3.3. 2005.

(30) van der Spoel, D.; Lindahl, E.; Hess, B.; Groenhof, G.; Mark, A. E.; Berendsen, H. J. C. *J. Comput. Chem.* **2005**, *26*, 1701–1718.

(31) Hess, B.; Kutzner, C.; van der Spoel, D.; Lindahl, E. *J. Chem. Theory Comput.* **2008**, *4*, 435–447.

(32) Berendsen, H. J. C.; Postma, J. P. M.; van Gunsteren, W. F.; DiNola, A.; Haak, J. R. *J. Chem. Phys.* **1984**, *81*, 3684–3690.

(33) Bussi, G.; Donadio, D.; Parrinello, M. *J. Chem. Phys.* **2007**, *126*, 014101.

(34) Hockney, R. W.; Goel, S. P.; Eastwood, J. W. *J. Comput. Phys.* **1974**, *14*, 148–158.

(35) Essmann, U.; Perera, L.; Berkowitz, M. L.; Darden, T.; Lee, H.; Pedersen, L. G. *J. Chem. Phys.* **1995**, *103*, 8577–8592.

(36) Haughney, M.; Ferrario, M.; McDonald, I. R. *J. Phys. Chem.* **1987**, *91*, 4934–4940.

(37) Schnabel, T. Molecular modeling and simulation of hydrogen bonding pure fluids and mixtures. Ph.D. thesis, Institut für Technische Thermodynamik und Thermische Verfahrenstechnik, Universität Stuttgart, 2008.

(38) Humphrey, W.; Dalke, A.; Schulten, K. *J. Mol. Graph.* **1996**, *14*, 33–38.

(39) Grottel, S.; Reina, G.; Dachsbacher, C.; Ertl, T. *Comput. Graph. Forum* **2010**, *29*, 953–962.

(40) Thomaß, B.; Walter, J.; Krone, M.; Hasse, H.; Ertl, T. Interactive Exploration of Polymer-Solvent Interactions. 2011.

(41) Walter, J.; Deublein, S.; Vrabec, J.; Hasse, H. In *High Performance Computing in Science and Engineering '09*; Nagel, W. E., Kröner, D. B., Resch, M. M., Eds.; Springer, Berlin, 2010; Chapter Chemistry, Development of Models for Large Molecules and Electrolytes in Solution for Process Engineering, pp 165–176.

Table 1: Characterization of the present hydrogel synthesis: Total mass fraction x^m_{gel} of polymerizable material, mole fraction of cross-linking agent x^n_{MBA} and mass fraction of the initiator x^m_{s}. The two hydrogels differ mainly in the degree of cross-linking.

Hydrogel	x^m_{gel} / g·g^{-1}	x^n_{MBA} / mol·mol^{-1}	x^m_{s} / g·g^{-1}
1	0.0800	0.02	$4.244 \cdot 10^{-4}$
2	0.0797	0.01	$4.186 \cdot 10^{-4}$

Table 2: Degree of swelling q of Hydrogel 1 ($x^m_{\mathrm{MBA}} = 0.02$ g·g^{-1}, cf. 1) in water/methanol mixtures as a function of the mole fraction of methanol $\mathrm{x}^n_{\mathrm{MeOH}}$ at three temperatures. The numbers behind $\pm$ denote the standard deviation.

$\mathrm{x}^n_{\mathrm{MeOH}}$ / mol·mol^{-1}	q / g·g^{-1}		
	268.15 K	298.15 K	313.15 K
0.000	-	24.04 ± 0.56	1.77 ± 0.08
0.100	34.52 ± 2.02	11.44 ± 0.65	1.70 ± 0.04
0.200	23.70 ± 1.45	1.93 ± 0.04	2.04 ± 0.09
0.300	9.15 ± 0.24	2.37 ± 0.03	2.31 ± 0.04
0.400	9.72 ± 0.41	4.35 ± 0.15	3.56 ± 0.06
0.500	14.97 ± 0.88	11.63 ± 0.61	12.56 ± 0.55
0.601	18.92 ± 0.36	16.69 ± 0.21	17.19 ± 0.39
0.700	20.91 ± 0.41	19.69 ± 0.35	19.38 ± 0.22
0.800	22.35 ± 0.39	21.05 ± 0.29	20.61 ± 0.26
0.902	22.34 ± 0.73	21.34 ± 0.24	20.65 ± 0.70
1.000	21.96 ± 0.65	20.76 ± 0.53	19.91 ± 0.23

Table 3: Degree of swelling q of Hydrogel 2 ($x^m_{\mathrm{MBA}} = 0.01$ **g·g^{-1}, cf. 1) in water/methanol mixtures as a function of the mole fraction of methanol $\mathrm{x}^n_{\mathrm{MeOH}}$ at three temperatures. The numbers behind $\pm$ denote the standard deviation.**

$\mathrm{x}^n_{\mathrm{MeOH}}$ / mol·mol^{-1}	q / g·g^{-1}		
	268.15 K	298.15 K	313.15 K
0.000	-	34.02 ± 1.28	1.54 ± 0.05
0.100	58.73 ± 1.55	1.91 ± 0.06	1.58 ± 0.06
0.200	50.43 ± 1.81	2.10 ± 0.04	1.78 ± 0.04
0.300	7.41 ± 0.60	2.58 ± 0.11	2.21 ± 0.02
0.400	9.02 ± 0.75	5.24 ± 0.31	4.72 ± 0.06
0.500	20.52 ± 0.51	17.81 ± 0.67	16.68 ± 0.52
0.601	26.09 ± 0.56	24.76 ± 0.62	23.35 ± 0.65
0.700	29.10 ± 1.29	27.00 ± 1.60	27.67 ± 0.34
0.800	30.43 ± 1.24	29.04 ± 0.88	29.16 ± 0.59
0.902	30.76 ± 1.25	30.59 ± 0.48	29.88 ± 0.51
1.000	30.75 ± 1.02	29.01 ± 1.02	28.69 ± 0.48

Table 4: Transition points $x^{n,*}_{\mathrm{MeOH}}$ for Hydrogel 1 ($x^m_{\mathrm{MBA}} = 0.02$ **g·g^{-1}) and Hydrogel 2 ($x^m_{\mathrm{MBA}} = 0.01$ **g·g^{-1}**) as estimated with the empirical procedure described in the text: Relation between temperature and methanol mole fraction x^n_{MeOH}. If two values are listed, cononsolvency was observed. Starting from small methanol mole fractions, the lower number corresponds to the collapse upon passing the threshold, the higher number to the swelling.**

Hydrogel	$x^{n,*}_{\mathrm{MeOH}}$ / mol·mol^{-1}		
	268.15 K	298.15 K	313.15 K
1	0.30 / 0.38	0.08 / 0.43	0.43
2	0.30 / 0.40	0.12 / 0.47	0.47

Table 5: Lennard-Jones parameters (σ and ε) and point charge magnitude (q_{el}) of the PNI-PAAm force field OPLS,[22,23] where e is the elementary charge.

site	OPLS		
	σ / nm	ε / kJ·mol^{-1}	q_{el} / e
C	0.375	0.4393	0.50
O	0.296	0.8786	-0.50
N	0.325	0.7113	-0.50
H	-	-	0.30
CH(-N)	0.350	0.2761	0.14
CH	0.350	0.2761	-0.06
CH_2	0.350	0.2761	-0.12
CH_3	0.350	0.2761	-0.18
H in CH_x	-	-	0.06

Table 6: Lennard-Jones parameters σ and ε and point charge magnitude q_{el} of the methanol model G96-low,[27] where e is the elementary charge.

Site	σ / nm	ε / kJ·mol^{-1}	q_{el} / e
CH_3	0.3552	1.1038	0.290
O	0.3143	0.6785	-0.690
H	-	-	0.400

Table 7: Bond and angle parameters, i.e. distances r, angles α and force constants of the harmonic potentials k of the methanol model G96-low.[27]

$r_{\mathrm{C-O}}$ nm	$k_{b,\mathrm{C-O}}$ kJ·mol^{-1}nm^{-2}	$r_{\mathrm{O-H}}$ nm	$k_{b,\mathrm{O-H}}$ kJ·mol^{-1}nm^{-2}	$\alpha_{\mathrm{C-O-H}}$	$k_{\alpha,\mathrm{C-O-H}}$ kJ·mol^{-1}rad^{-2}
0.136	376560	0.100	313800	108.53°	397.5

Table 8: Radius of gyration R_g of a PNIPAAm chain of 30 monomers in water/methanol mixtures in equilibrium as a function of the methanol mole fraction x^n_{MeOH} at three different temperatures. The numbers behind $\pm$ denote the standard deviation.

x^n_{MeOH} / mol·mol^{-1}	R_g / nm		
	268 K	298 K	330 K
0.000	-	1.92 ± 0.05	1.11 ± 0.03
0.110	-	1.11 ± 0.04	-
0.202	1.73 ± 0.05	1.05 ± 0.05	1.19 ± 0.07
0.297	-	1.59 ± 0.12	-
0.411	1.58 ± 0.12	1.74 ± 0.07	1.27 ± 0.09
0.487	1.84 ± 0.06	-	1.45 ± 0.17
0.579	1.23 ± 0.07	1.79 ± 0.08	1.68 ± 0.08
0.692	1.71 ± 0.11	-	-
0.790	1.79 ± 0.06	1.70 ± 0.01	1.63 ± 0.10
1.000	1.66 ± 0.09	1.76 ± 0.08	1.46 ± 0.13

Table 9: Average number of H-bonds between methanol or water and the oxygen or hydrogen atom of the amide group of a monomer unit of the PNIPAAm chain for a solvent methanol mole fraction of 0.1 mol·mol^{-1}.

PNIPAAm	methanol	water
O	0.41	0.75
H	0.39	0.22

Figure 1: Degree of swelling q of the PNIPAAm Hydrogel 1 ($x^m_{\mathrm{MBA}} = 0.02$ mol·mol^{-1}) in water/methanol mixtures at 268.15 K (○), 298.15 K (▽), and 313.15 K (□) as a function of the mole fraction of methanol x^n_{MeOH}. Symbols: experimental data from this work, lines: guide for the eye. The error bars denote the standard deviation.

Figure 2: Degree of swelling q of the PNIPAAm Hydrogel 1 ($x^m_{\mathrm{MBA}} = 0.02$ mol·mol^{-1}) (○), and Hydrogel 2 ($x^m_{\mathrm{MBA}} = 0.01$ mol·mol^{-1}) (▽) in water/methanol mixtures as a function of the mole fraction of methanol x^n_{MeOH} at 298.15 K. Symbols: experimental data from this work, lines: guide for the eye. The error bars denote the standard deviation.

Figure 3: Comparison of transition points of PNIPAAm in water/methanol mixtures determined in different ways: Estimates from the present experimental results for PNIPAAm Hydrogel 1 ($x^m_{\mathrm{MBA}} = 0.02$ g·g^{-1}) (□) and Hydrogel 2 ($x^m_{\mathrm{MBA}} = 0.01$ g·g^{-1}) (▽) and experimental cloud point data for PNIPAAm polymers by Winnik et al.[17] (●).

Figure 4: Radius of gyration R_g of a PNIPAAm chain of 30 monomers in water/methanol mixtures in equilibrium as a function of the methanol mole fraction x^n_{MeOH} at 268, 298 and 330 K. The error bars indicate the standard deviation. There are no results for pure water at 268 K, because it is solid at this temperature.

Figure 5: Average number of H-bonds between methanol (▽) and water (□) and a monomer unit of the PNIPAAm chain as a function of the methanol mole fraction x^n_{MeOH} at 298 K and 1 bar. Additionally, the radius of gyration R_g (–) is shown as well as linear interpolations between the number of H-bonds for the pure solvents methanol (– –) and water ($\cdots$) and zero where the solvent is not present in the mixture.

Figure 6: Snapshot of a PNIPAAm monomer from simulation. The colors indicate atom types:

carbon (black), hydrogen (white), oxygen (red) and nitrogen (blue). The upper two carbon atoms are part of the polymer backbone, denoted by the black tubes. The lower three carbon atoms are the non-polar end of the side group. In between these two sites are the four atoms of the polar amide group, which forms H-bonds with the solvent molecules.

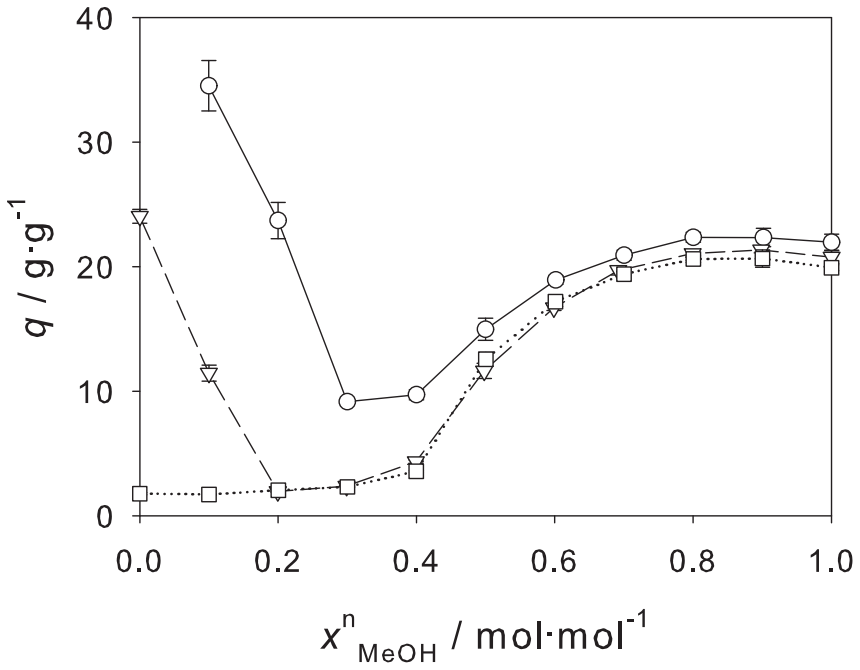

Figure 1

This material is available free of charge via the Internet at `http://pubs.acs.org/`.

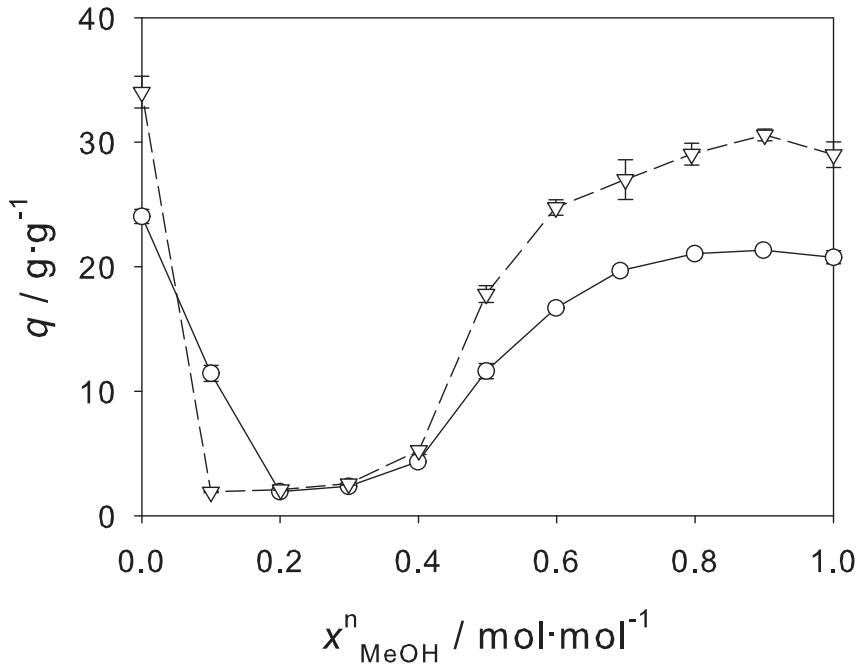

Figure 2

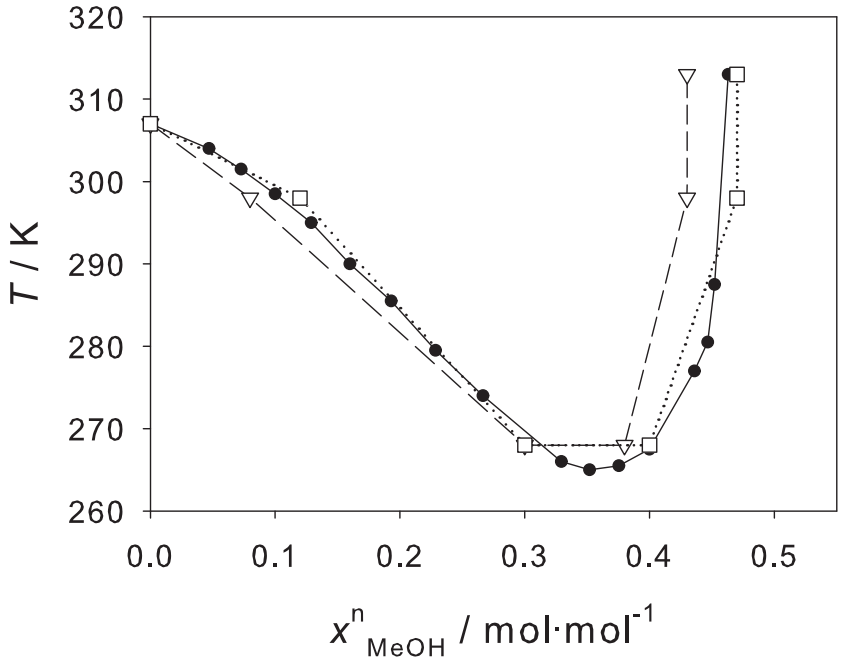

Figure 3

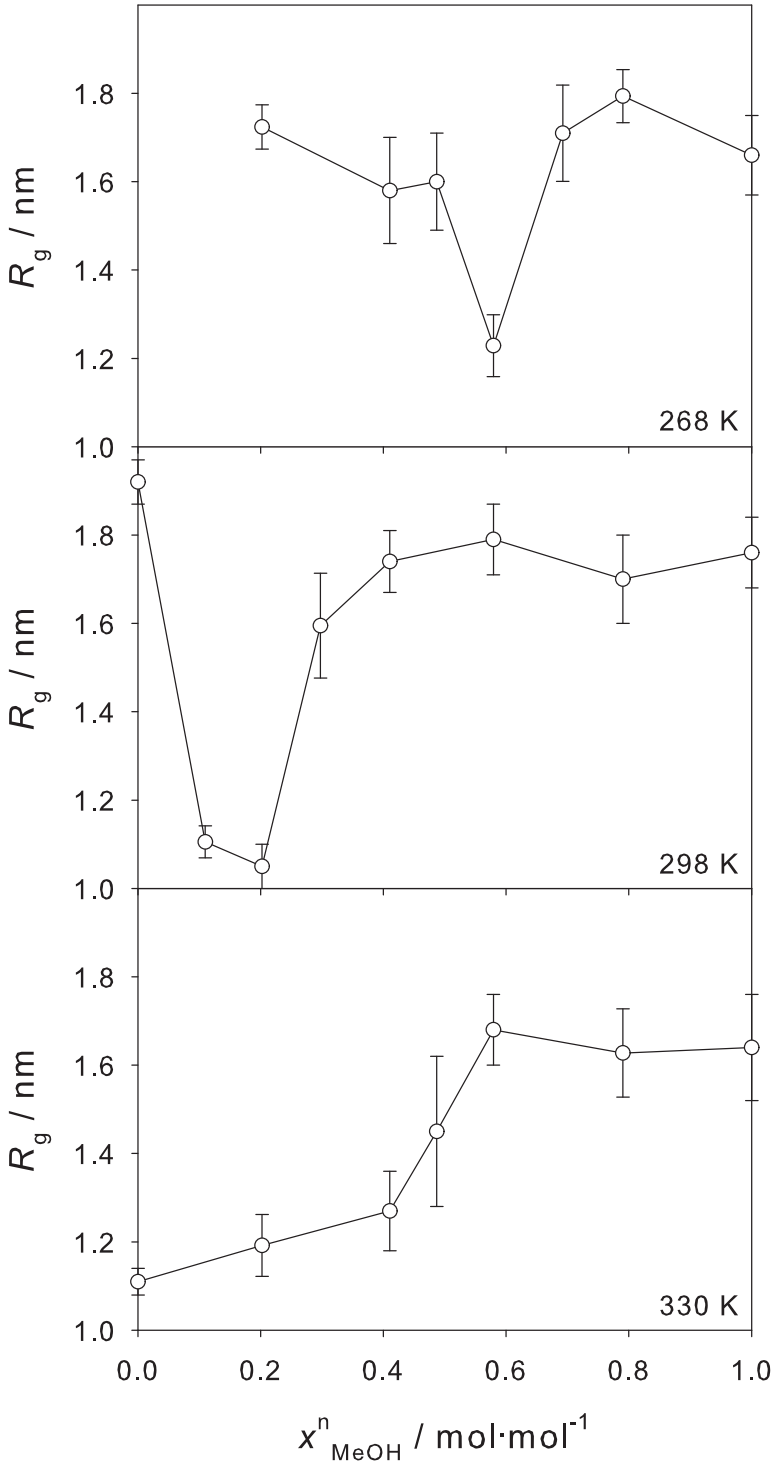
R_g / nm
1.0
1.2
1.4
1.6
1.8
268 K
298 K
330 K
0.0
0.2
0.4
0.6
0.8
1.0
x^n_{MeOH} / mol·mol^{-1}

Figure 4

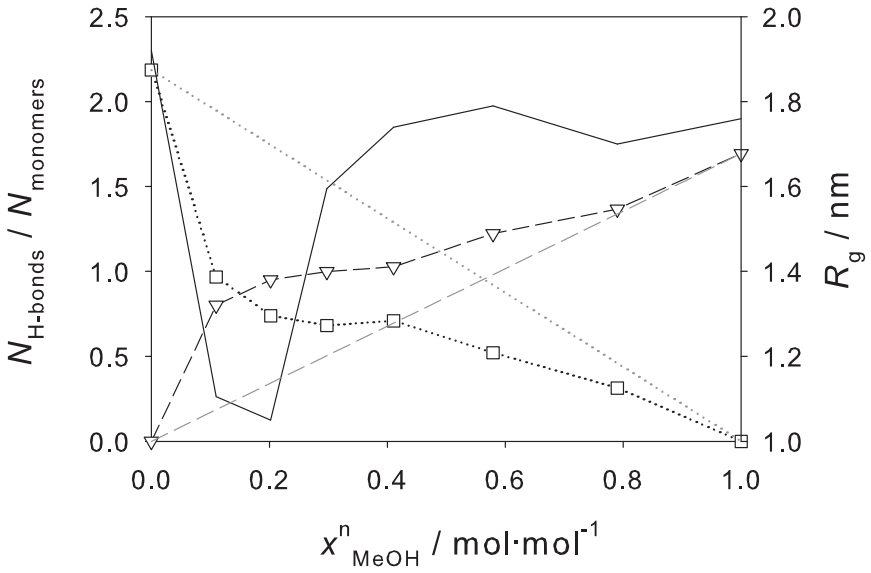

Figure 5

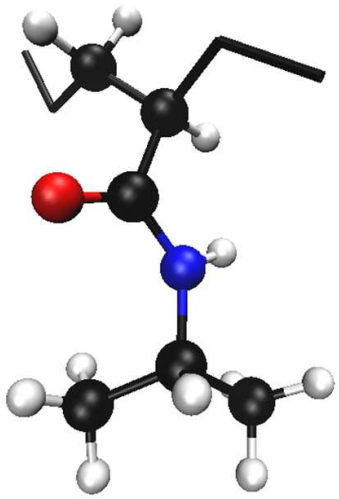

Figure 6

Molecular Dynamics and Experimental Study of Conformation Change of Poly(N-isopropylacrylamide)-hydrogels in Mixtures of Water and Methanol

Jonathan Walter,[†] Jan Sehrt,[†] Jadran Vrabec,[‡] and Hans Hasse[*,†]

Laboratory of Engineering Thermodynamics, University of Kaiserslautern, Kaiserslautern, Germany, and Thermodynamics and Energy Technology, University of Paderborn, Paderborn, Germany

E-mail: hans.hasse@mv.uni-kl.de

Appendix A: Applicability of different methanol models

In order to find a suitable methanol model for the simulations of PNIPAAm in water/methanol mixtures, in a preliminary study three methanol models from the literature were tested: Schnabel et al. (Schnabel),[1] GROMOS96 with high (G96-high) and with low (G96-low) point charges.[2] The Schnabel model is a rigid body, the two G96 models consider the internal degrees of freedom. In all three models, CH_3 is described by one united-atom site.

The methanol model Schnabel was developed using the Lorentz-Berthelot mixing rule,[3,4] i.e. the

[†]University of Kaiserslautern
[‡]University of Paderborn

arithmetic mean for σ and the geometric mean for ε. The OPLS force field was developed using the geometric mean both for σ and ε.[5,6]

In a first step, simulations with the three methanol models were carried out for liquid water/methanol mixtures at 298 K and 1 bar to determine the density. Figure S1 presents the results for water/methanol mixtures for the different methanol models in comparison to experimental data.[7] The density ρ from simulation is plotted as a function of the methanol mole fraction x^n_{MeOH}. The methanol model Schnabel shows the best and G96-high[2] the worst agreement with the experimental data. The values for the methanol model G96-low[2] are in between.

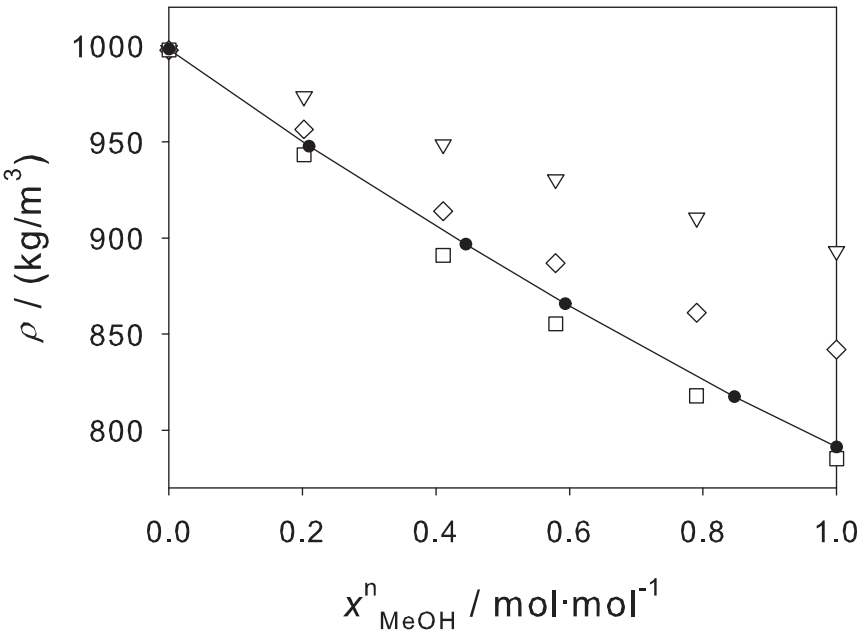

Figure S1: Density ρ of water/methanol mixtures at 298.15 K and 1 bar as a function of the methanol mole fraction x^n_{MeOH} in comparison with experimental data[7] (●) at 298.15 K and 1 bar for the three methanol models: Schnabel[1] (□), G96-low (◇) and G96-high[2] (▽). The water model was always SPC/E.

In a second step, a PNIPAAm single chain was simulated in water/methanol mixtures at 298 K with all three methanol models. For this temperature, the hydrogel is swollen in the pure solvents and shows a cononsolvency region in the water-rich mixture. Therefore, the single chain should be stretched in both pure solvents and collapsed in water-rich mixtures. All three methanol models

yielded the stretched conformation in the pure solvents. However, only the G96-low model was able to predict cononsolvency of the PNIPAAm chain. Therefore, this model was used for all further investigations of the swelling behavior of PNIPAAm chains in water/methanol mixtures.
The methanol model Schnabel[1] is clearly the best for predicting the density of the liquid mixture. The fact that it is not suited for predicting cononsolvency of PNIPAAm in water/methanol mixtures may be due to incompatible mixing rules for the OPLS force field and for that model.

Appendix B: H-bond statistics

Figure S2 shows the average number of H-bonds between the solvent molecules (methanol or water) and the two atoms of the amide group (oxygen and hydrogen) of the PNIPAAm chain as a function of the methanol mole fraction at 298 K. In pure water, more H-bonds are present between the solvent and the two PNIPAAm atoms than in pure methanol. Except for the water-rich region of water/methanol mixtures, the number of H-bonds is almost constant and the same as in pure methanol. The ratio of H-bonds formed by the oxygen atom and those formed by the hydrogen atom of PNIPAAm is around two for all solvent compositions. For pure water, Tanaka et al.[8] measured two H-bonds between water and the oxygen atom of PNIPAAm and one H-bond with the hydrogen atom leading to the same ratio as seen in the present simulations.
Furthermore, it can be seen that the number of H-bonds between the solvent and PNIPAAm is not decreasing in the cononsolvency region. This leads to the conclusion that PNIPAAm is not dehydrated in the collapsed conformation, which supports the findings of Cheng et al.[9]
The average number of H-bonds between methanol and the two atoms of the amide group (oxygen and hydrogen) as well as water and the two atoms (oxygen and hydrogen) of the PNIPAAm chain as a function of the methanol mole fraction at 298 K and 1 bar is presented in Figure S3 and Table S1. In addition to the conclusions from Figure 5 in the main manuscript and Figure S2, the preference of water for the oxygen atom and of methanol for the hydrogen atom of the amide group can be seen here. At methanol mole fractions between 0.2 and 0.4 mol·mol^{-1}, the number

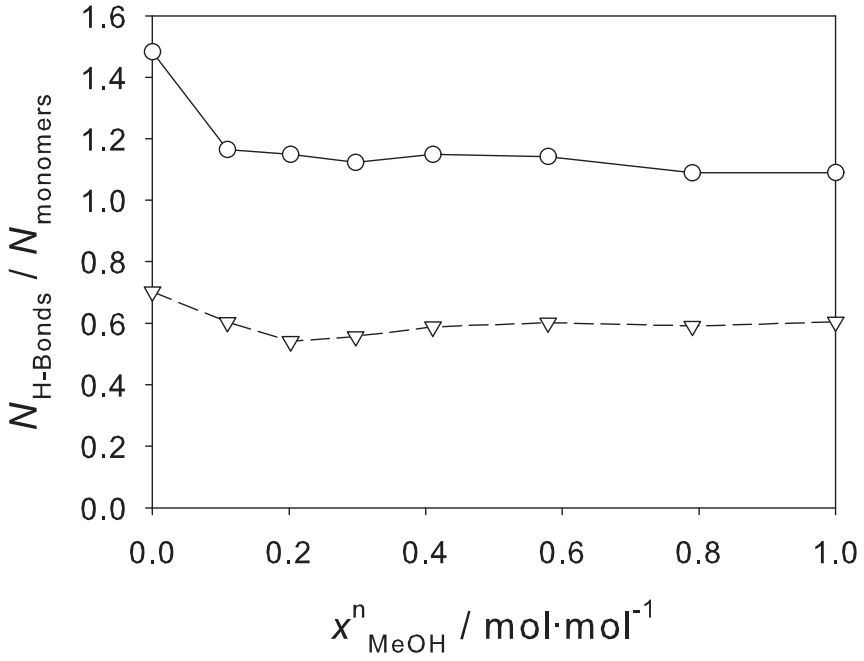

Figure S2: Average number of H-bonds between the solvent molecules (methanol or water) and the two atoms of the amide group oxygen (○) and hydrogen (▽) of the PNIPAAm chain as a function of the methanol mole fraction x^{n}_{MeOH} at 298 K and 1 bar.

of H-bonds between the oxygen atom and water is almost equal to the number of H-bonds between the oxygen atom and methanol. However, in the same composition range, the number of H-bonds between the hydrogen atom and methanol is more than twice as high as the number of H-bonds between the hydrogen atom and water.

Appendix C: Visualization

For the simulations at 298 K and methanol mole fractions of 0.0, 0.4 and 1.0 mol·mol^{-1}, visualizations were performed using VMD.[10] In these visualizations, the backbone and five monomers of the PNIPAAm chain are displayed together with the hydration shell around these monomer units, cf. Supplementary Material. The studied scenario is a polymer chain in equilibrium.

In these visualizations, the structure of the solvent shell at the surface of the PNIPAAm chain can be seen. In pure water, the solvent is strongly structured and the H-bonds are more stable than

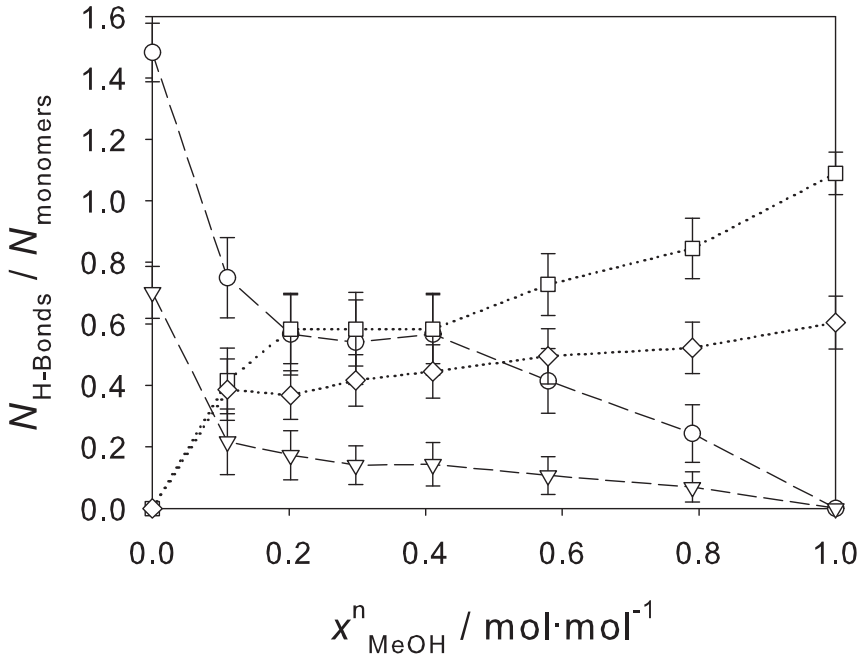

Figure S3: Average number of H-bonds between the water (– –) and the two atoms oxygen (○) and hydrogen (▽) of the amide group as well as methanol (···) and the two atoms oxygen (□) and hydrogen (◇) of the PNIPAAm chain as a function of the methanol mole fraction x^n_{MeOH} at 298 K and 1 bar. The error bars denote the standard deviation.

Table S1: Average number of H-bonds between methanol and the two atoms oxygen and hydrogen of the amide group as well as water and the two atoms oxygen and hydrogen of the PNIPAAm chain as a function of the methanol mole fraction x^n_{MeOH} at 298 K and 1 bar. The numbers behind ± denote the standard deviation.

x^n_{MeOH} / mol·mol^{-1}	H-bonds			
	H$_2$O - **O**	H$_2$**O** - **H**	Me**O**H - **O**	Me**O**H - **H**
0.000	1.48 ± 0.10	0.70 ± 0.08	-	-
0.110	0.75 ± 0.13	0.22 ± 0.11	0.41 ± 0.11	0.39 ± 0.10
0.202	0.57 ± 0.13	0.17 ± 0.08	0.58 ± 0.11	0.37 ± 0.08
0.297	0.54 ± 0.14	0.14 ± 0.06	0.58 ± 0.12	0.42 ± 0.08
0.411	0.57 ± 0.13	0.14 ± 0.07	0.58 ± 0.11	0.45 ± 0.09
0.579	0.41 ± 0.11	0.11 ± 0.06	0.73 ± 0.10	0.49 ± 0.09
0.790	0.24 ± 0.09	0.07 ± 0.05	0.85 ± 0.10	0.52 ± 0.08
1.000	-	-	1.09 ± 0.07	0.60 ± 0.09

in pure methanol. This is in agreement with the findings of Winnik et al.[11] In the visualization for the methanol concentration of 0.4 mol·mol^{-1}, it can be seen that the water molecules in the solvent shell are typically closer to the PNIPAAm backbone than the methanol molecules. It can also be seen that the methanol molecules in the solvent shell are oriented such that their non-polar methyl-group is directed to the surrounding bulk solvent, thereby shielding the polar sites of the PNIPAAm chain.

In other simulations, also instationary processes were studied and visualized. These visualizations were performed with MegaMol.[12] The amount of methanol in the hydration shell of the polymer was displayed in a dynamical way. For details of these visualizations see Thomaß et al.[13] The simulation starts with a methanol mole fraction in the whole simulation volume of 0.1 mol·mol^{-1} at 298 K, which is in the cononsolvency region. In this simulation, methanol is very quickly enriched in the solvent shell. This leads to a methanol mole faction of about 0.44 mol·mol^{-1} in the solvation shell. Upon increase of the methanol concentration in the solvent shell, the polymer starts to collapse. This visualization is also included in the Supplementary Material.

References

(1) Schnabel, T.; Srivastava, A.; Vrabec, J.; Hasse, H. *J. Phys. Chem. B* **2007**, *111*, 9871–9878.

(2) van Gunsteren, W. F.; Billeter, S.; Eising, A.; Hünenberger, P.; Krüger, P.; Mark, A.; Scott, W.; Tironi, I. *Biomolecular Simulation: The Gromos 96 Manual and User Guide*; vdf Hochschulverlag an der ETH Zürich: Zürich, Switzerland, 1996.

(3) Lorentz, H. A. *Ann. Phys.* **1881**, *12*, 127–136.

(4) Berthelot, D. *C. R. Acad. Sci.* **1898**, *126*, 1703–1706.

(5) Jorgensen, W. L.; Tirado-Rives, J. *J. Am. Chem. Soc.* **1988**, *110*, 1657–1666.

(6) Jorgensen, W. L.; Maxwell, D. S.; Tirado-Rives, J. *J. Am. Chem. Soc.* **1996**, *118*, 11225–11236.

(7) Zarei, H. A.; Jalili, F.; Assadi, S. *J. Chem. Eng. Data* **2007**, *52*, 2517–2526.

(8) Tanaka, F.; Koga, T.; Kojima, H.; Winnik, F. M. *Macromolecules* **2009**, *42*, 1321–1330.

(9) Cheng, H.; Shen, L.; Wu, C. *Macromolecules* **2006**, *39*, 2325–2329.

(10) Humphrey, W.; Dalke, A.; Schulten, K. *J. Mol. Graph.* **1996**, *14*, 33–38.

(11) Winnik, F. M.; Ringsdorf, H.; Venzmer, J. *Macromolecules* **1990**, *23*, 2415–2416.

(12) Grottel, S.; Reina, G.; Dachsbacher, C.; Ertl, T. *Comput. Graph. Forum* **2010**, *29*, 953–962.

(13) Thomaß, B.; Walter, J.; Krone, M.; Hasse, H.; Ertl, T. Interactive Exploration of Polymer-Solvent Interactions. *Proc. Vision, Modeling and Visualization '11*, 2011; pp 301–308.